Received: 17 July 2021 | Revised: 12 October 2021 | Accepted: 21 October 2021

DOI: 10.1002/hbm.25708

RESEARCH ARTICLE

WILEY

Intermittent theta burst stimulation over the parietal cortex has a significant neural effect on working memory

Xinping Deng[1] | Jue Wang[2] | Yufeng Zang[3,4,5] | Yang Li[1] | Wenjin Fu[1] | Yanyan Su[1] | Xiongying Chen[6] | Boqi Du[1] | Qi Dong[1] | Chuansheng Chen[7] | Jun Li[1]

[1]State Key Laboratory of Cognitive Neuroscience and Learning & IDG/McGovern Institute for Brain Research, Beijing Normal University, Beijing, China

[2]Institute of Sports Medicine and Health, Chengdu Sport University, Chengdu, China

[3]Center for Cognition and Brain Disorders, The Affiliated Hospital of Hangzhou Normal University, Hangzhou, China

[4]Institute of Psychological Sciences, Hangzhou Normal University, Hangzhou, China

[5]Zhejiang Key Laboratory for Research in Assessment of Cognitive Impairments, Hangzhou, China

[6]The National Clinical Research Center for Mental Disorders & Beijing Key Laboratory of Mental Disorders & the Advanced Innovation Center for Human Brain Protection, Beijing Anding Hospital, School of Mental Health, Capital Medical University, Beijing, China

[7]Department of Psychological Science, University of California, Irvine, California, USA

Correspondence
Jun Li, State Key Laboratory of Cognitive Neuroscience and Learning & IDG/McGovern Institute for Brain Research, Beijing Normal University, Beijing, China.
Email: lijundp@bnu.edu.cn

Funding information
National Natural Science Foundation of China, Grant/Award Number: 31771242

Abstract

The crucial role of the parietal cortex in working memory (WM) storage has been identified by fMRI studies. However, it remains unknown whether repeated parietal intermittent theta-burst stimulation (iTBS) can improve WM. In this within-subject randomized controlled study, under the guidance of fMRI-identified parietal activation in the left hemisphere, 22 healthy adults received real and sham iTBS sessions (five consecutive days, 600 pulses per day for each session) with an interval of 9 months between the two sessions. Electroencephalography signals of each subject before and after both iTBS sessions were collected during a change detection task. Changes in contralateral delay activity (CDA) and *K*-score were then calculated to reflect neural and behavioral WM improvement. Repeated-measures ANOVA suggested that real iTBS increased CDA more than the sham one ($p = .011$ for iTBS effect). Further analysis showed that this effect was more significant in the left hemisphere than in the right hemisphere ($p = .029$ for the hemisphere-by-iTBS interaction effect). Pearson correlation analyses showed significant correlations for two conditions between CDA changes in the left hemisphere and *K* score changes (*p*s <.05). In terms of the behavioral results, significant *K* score changes after real iTBS were observed for two conditions, but a repeated-measures ANOVA showed a nonsignificant main effect of iTBS ($p = .826$). These results indicate that the current iTBS protocol is a promising way to improve WM capability based on the neural indicator (CDA) but further optimization is needed to produce a behavioral effect.

KEYWORDS
contralateral delay activity, parietal cortex, theta burst stimulation, working memory

1 | INTRODUCTION

Working memory (WM) is a cognitive process that allows temporary storage and manipulation of information relevant to the ongoing or upcoming behaviors. It makes important contributions to more complex cognitive processes such as counting, reading, problem solving, and planning (Duncan & Owen, 2000; Goel & Grafman, 2000; Rypma, Prabhakaran, Desmond, & Gabrieli, 2001), and its impairment has

been linked to some mental disorders such as schizophrenia and Alzheimer's disease. Although the typical WM capacity is 3–4 items/chunks (Cowan, 2001; Luck & Vogel, 1997), researchers have been interested in improving WM via cognitive training (Constantinidis & Klingberg, 2016), medicine (Cools & D'Esposito, 2011), and stimulation methods such as repetitive transcranial magnetic stimulation (rTMS; Brunoni & Vanderhasselt, 2014).

rTMS is a noninvasive brain stimulation (NIBS) technique that applies brief, high intensity magnetic field pulses to the scalp, either during (online) or before (off-line) the performance of a cognitive task. A number of rTMS WM studies have targeted the prefrontal cortex because it is the main part of the frontoparietal network for WM (D'Esposito & Postle, 2015; Feredoes, Heinen, Weiskopf, Ruff, & Driver, 2011; Xu, 2017). However, the results have been mixed (Bagherzadeh, Khorrami, Zarrindast, Shariat, & Pantazis, 2016; Hoy et al., 2016; Vékony et al., 2018). To our knowledge, 17 studies have tested the effect of prefrontal rTMS on WM, with five of them reporting beneficial effects while the remaining 12 studies reporting nonsignificant or even harmful effects. Indeed, a recent meta-analysis concluded that NIBS including rTMS over the prefrontal cortex, either online or offline, could not improve WM (de Boer et al., 2021).

As the other key node within the frontoparietal network, the parietal cortex plays a unique and important role in WM capacity. Previous fMRI studies showed that brain activation within the parietal cortex increased linearly with the number of memorized items and reached its asymptote when WM capacity was exhausted (Hahn, Robinson, Leonard, Luck, & Gold, 2018; Todd, Marois, & Todd, 2004; Xu & Chun, 2006). Similarly, electroencephalography (EEG) studies found that, contralateral delay activity (CDA), a component that originates from the parietal cortex (Becke, Müller, Vellage, Schoenfeld, & Hopf, 2015; Brigadoi et al., 2017; Robitaille, Grimault, & Jolicœur, 2009), also showed such patterns (Luck & Vogel, 2013; Vogel & Machizawa, 2004). Therefore, the parietal cortex is also a candidate target of rTMS to improve WM. Indeed, some studies in healthy adults have tested the effects of parietal rTMS on WM. Most of these studies used online rTMS and found that 5–10 Hz rTMS produced immediate but no lasting effects on WM (Albouy, Weiss, Baillet, & Zatorre, 2017; Hamidi, Tononi, & Postle, 2008; Li et al., 2017; Luber et al., 2007; Riddle, Scimeca, Cellier, Dhanani, & D'Esposito, 2020; Sauseng et al., 2009; Yamanaka, Yamagata, Tomioka, Kawasaki, & Mimura, 2010). However, rTMS with frequency higher than 10 Hz such as 15 and 25 Hz (Kessels, D'Alfonso, Postma, & De Haan, 2000; Sauseng et al., 2009), lower than 5 Hz (Postle et al., 2006) or single pulse (Oliveri et al., 2001) was not effective or was even harmful to WM.

Although a large number of studies have used online rTMS to target the parietal cortex, few studies have used offline rTMS, which is believed to induce longer lasting effects than does online rTMS. Thus far, only two studies (Morgan, Jackson, Van Koningsbruggen, Shapiro, & Linden, 2013; Praß & de Haan, 2019) have examined the effect of parietal offline-rTMS on WM. Both reported that offline-rTMS using continuous theta-burst stimulation (cTBS) (5 Hz bursts with each burst containing three pulses at 50 Hz) had harmful effects on WM (Morgan et al., 2013; Praß & de Haan, 2019). In contrast to the cTBS's inhibitory role, intermittent TBS (iTBS, delivered in 2 s trains followed by 8 s rest for a total of 192 s) should be facilitatory (Di Lazzaro et al., 2008; Di Lazzaro, Huang et al., 2005; Ziemann, & Lemon, 2008). However, no study has examined whether iTBS would facilitate parietal excitability and hence improve WM.

The current study aimed to test the effect of parietal iTBS on WM. We recruited 30 healthy adults, who received two 5-day iTBS sessions (real and sham) that were arranged in a randomized order and with an interval of 9 months. We applied iTBS to each subject under the guidance of his (or her) own fMRI brain activation map within the left parietal cortex (Riddle et al., 2020; Sack et al., 2009) and recorded EEG signals of each subject before and after each iTBS session. We then compared the effects of real and sham iTBS on the neural index (changes in CDA) and the behavioral index (changes in *K* score) of WM improvement. The change detection task that we used included three conditions (three targets to be remembered, 3T; three targets plus two distractors, 3T2D; five targets without distractor, 5T). In addition to using CDA amplitude at each condition to reflect WM maintenance process, the relative CDA amplitudes across the three conditions, which has been suggested to reflect an individual's capability of interference control (Vogel, McCollough, & Machizawa, 2005), were also analyzed. We hypothesized that parietal iTBS would increase CDA and *K* score.

2 | MATERIALS AND METHODS

2.1 | Subjects

This was a within-subject randomized controlled study. Thirty (12 males and 18 females) healthy undergraduate and graduate students (mean education = 15 ± 1.96 years), aged between 18 to 26 years old (mean age = 21 ± 2.43 years) were recruited by internet advertisement. All subjects were interviewed by experienced psychiatrists to exclude current or previous psychiatric or neurological diseases. Subjects with contraindications to TMS or MRI were also excluded. All subjects had normal or corrected-to-normal vision and were right-handed. Subjects first received MRI scan which was used to localize their peak locations within the left parietal cortex for WM capacity, and then finished two iTBS sessions (real and sham) which were arranged according to a computer-generated random number list. They received four EEG assessments (prereal iTBS, postreal iTBS, presham iTBS, and postsham iTBS). For each iTBS session (either real or sham), the pretest was administered 1 day before the first iTBs and the posttest 1 day after the fifth iTBS. All subjects finished their first iTBS session and corresponding assessment before the outbreak of COVID-19. The second iTBS session was administered when the outbreak of COVID-19 was alleviated in China. Eight subjects could not finish the second iTBS session due to the impact of COVID-19. As a result, data of 22 subjects were used in the final analyses.

This study was approved by the Beijing Normal University Institutional Review Board and registered on the Chinese Clinical Trial

Registry (ChiCTR2000040518). All subjects provided their written informed consents and were paid.

2.2 | fMRI data acquisition and data processing

Structural and functional MRI data were collected on a 3-T Siemens Magnetom Prisma scanner (Siemens, Erlangen, Germany) at the Brain Imaging Center of Beijing Normal University. Subjects did some practice on the fMRI task before they received an MRI scan. During scanning, subjects' heads were snugly fixed with straps and foam pads to restrict their movement. Functional images were collected first with the following multi-slice echo-planar imaging (EPI) sequence: repetition time (TR) = 2,000 ms; echo time (TE) = 30 ms; flip angle = 90°; field of view (FOV) = 200 × 200 mm^2; matrix size = 80 × 80; axial slices = 56; 2.5 mm slice thickness without gap (i.e., interleaved scan); voxel size = 2.5 × 2.5 × 2.5 mm^3. Afterward, axial T1-weighted images were acquired using a sagittal three dimensional (3D) magnetization-prepared rapid gradient echo sequence: TR = 2,530 ms; TE = 2.27 ms; flip angle = 7°; FOV = 256 × 256 mm^2; matrix size = 256 × 256; slices = 208; thickness = 1.0 mm; voxel size = 1 × 1 × 1 mm^3.

The task used during fMRI scan was revised from a previous study (Vogel et al., 2005). Stimuli were red bars (0.69° × 0.23°) with varied orientations (0°, 30°, 60 °, 90°, 120°, and 180°) and varied numbers (1 or 3), which resulted in two conditions (3T condition: three red bars as the targets [T] to be remembered, and 1T condition: 1 red bar as the target to be remembered). Each condition contained 30 trials. On each trial, a centrally placed black cross was presented first (for 200 ms, subjects were instructed to keep their eyes on it during the task), followed by a memory array (100 ms, subjects were instructed to remember the orientations of the red bars), a blank interval (1,900 ms, subjects were instructed to maintain the orientations of the red bars in their memory during this delay period) and a test array (1,800 ms, subjects were instructed to report whether the orientations of red bars were changed or not by pressing different response buttons).

The Statistical Parametric Mapping software (SPM12, Wellcome Department of Cognitive Neurology) was used for data processing. Preprocessing steps of functional images included slice-timing correction to the first slice, rigid-body realigning for motion correction (all subjects' head motion less than 2 mm in translation or 2° in rotation in any direction), functional/structural co-registration, resampling to a resolution of 3 × 3 × 3 mm^3, normalizing to MNI space using the EPI template, and spatial smoothing with a 6-mm FWHM Gaussian kernel.

We then used task condition (3T vs. 1T) as a predictor to produce whole brain activation images for each participant. In this analysis, a high-pass filter at 128 s was used to remove noise associated with low-frequency confounds. To achieve the peak voxel within the left parietal cortex, we limited the above analysis within the left parietal cortex mask that was defined by the Wake Forest University PickAtlas toolbox (WFU, http://fmri.wfubmc.edu/software/PickAtlas). For each subject, structural, activation, and mask images were transformed back into the native space, and the coordinates of the peak within the mask (threshold at p <.001) identified here would be used as the target in the following iTBS (as shown in Figure 1).

2.3 | EEG data acquisition and data processing

The EEG task was revised from the fMRI task. Stimuli were presented on a 21-in. gamma linearized CRT monitor (1,024 × 768 pixel, 120 Hz refresh rate) with a homogeneous gray background at a distance of 75 cm. Different from those used in the fMRI task, stimuli in the EEG task were red or blue bars that were presented bilaterally but subjects needed to remember only the stimuli on one side. As shown in Figure 2, this study included three conditions with 200 trials per condition. The three conditions, arranged as three blocks, included: three red bars as targets (T) with no distractor (3T), three red bars plus two blue bars as distractors (D) (3T2D), and five red bars with no distractor (5T). Specifically, each trial began with a centrally placed black cross (200 ms, subjects were instructed to keep their eyes on the black cross during the task), above which was an arrow directed to the left or the right. Afterward, a memory array (100 ms, subjects were instructed to remember the orientations of all the red bars at the side indicated by the arrow) and a test array (2,000 ms, subjects were instructed to report whether the orientations of all the red bars at the side indicated by the arrow were the same as those of the memory array) were presented on both sides of the cross in order. Between memory array and test array was an interval (900 ms) during which subjects were instructed to maintain their memory of the red bars' orientations. K score for each condition was calculated according to the formula suggested previously (Cowan, 2001; Pashler, 1988): $K = S \times (H - F)$, where S was the number of items to be remembered, H the

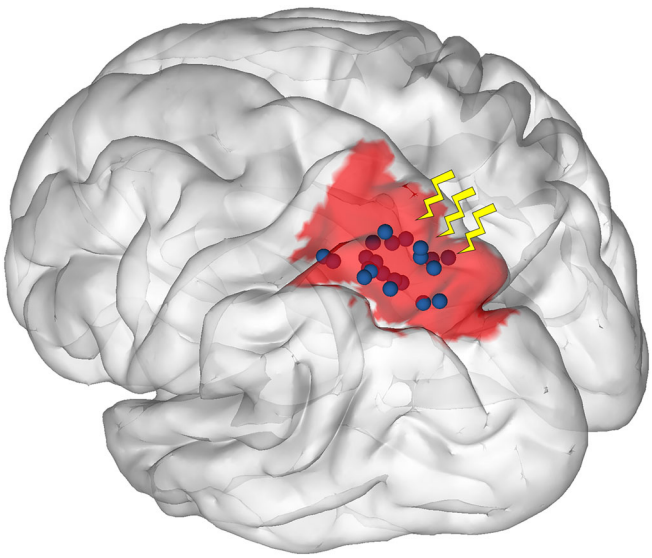

FIGURE 1 Distribution map for brain activation peak coordinates (rTMS stimulation target) within the left parietal cortex. The red shadow represents the left parietal mask that was produced using WFU software. Each sphere represents one subject

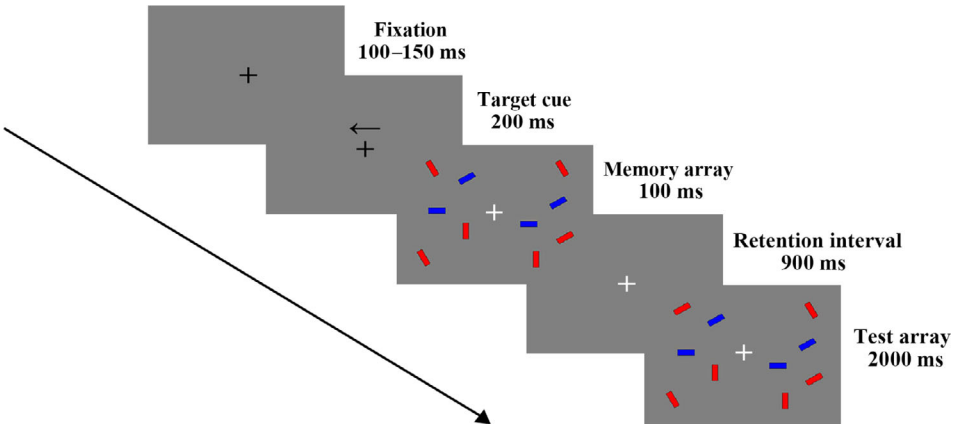

FIGURE 2 Schematic depiction of the EEG change detection task. Subjects were requested to remember the red targets but ignore the blue targets (if any) on the side indicated by the arrow. Three task conditions (3T, 3T2D, and 5T) were included. One condition (3T2D) is shown here as an example

hit rate, and *F* the rate of false alarm. A higher *K* score indicated better performance. *K* score for each condition was used in the final statistical analysis.

Subjects performed the experiment while sitting in a comfortable chair in a dim, electrically shielded chamber. EEG signals were recorded with a 64-channel SynAmps RT system (Neuroscan, El Paso, TX). Two vertical electrooculogram electrodes were placed both above and below the left eye to record vertical eye movements. Additional two horizontal electrooculogram electrodes were placed at the outer canthus of each eye to record horizontal eye movements. Except those for monitoring eye movements, all electrodes were referenced online to the left mastoid. Electrode impedance was kept well below 5 kΩ. EEG signals were filtered at 0.01–200 Hz and digitized online at a sampling rate of 500 Hz.

Offline EEG data processing was conducted in Matlab (The MathWorks Inc., Natick, MA) using the EEGLAB toolboxes (Delorme & Makeig, 2004) and custom codes. Preprocessing included down-sampling the data to 250 Hz, filtering the data by a 0.1–40 Hz bandpass filter, re-referencing data to the average of all the electrodes. After that, an independent component analysis (ICA) was conducted to remove components that were associated with eye-blink artifacts. Then, the EEG data were segmented into epochs with time locked to memory array onset (from −200 ms to 1,000 ms). Epochs were automatically rejected if the EEG exceeded ±75 μV at any electrode. Finally, EEG data were manually inspected to confirm that detection threshold was working as expected.

All the correctly responded trials were averaged for each condition to create the ERPs. We then focused on the ERP triggered by the memory array. Baseline correction was calculated using EEGs prior to the memory array. CDA was then calculated at POs and Os electrodes according to the method introduced by Vogel et al.'s (2005) study, with time window set at 300–900 ms after the onset of the memory array. In brief, CDA was calculated as the difference between the contralateral and the ipsilateral waveforms. The contralateral waveform was calculated by averaging the EEG activity across all right electrodes (PO4, PO6, PO8, and O2) when the to-be-remembered arrays were on the left side and the EEG activity across all left electrodes (PO3, PO5, PO7, and O1) when the to-be-remembered arrays were on the right side. The ipsilateral waveform was calculated by averaging the EEG activity across all right electrodes (PO4, PO6, PO8, and O2) when the to-be-remembered arrays were on the right side and the EEG activity across all left electrodes (PO3, PO5, PO7, and O1) when the to-be-remembered arrays were on the left side.

Considering the fact that only the left hemisphere received iTBS intervention, we also calculated hemispheric CDA (left CDA and right CDA). The left CDA was calculated by subtracting ERP of left-arrowed trials (ipsilateral) from ERP of right-arrowed trials (contralateral) and then averaged it across all left electrodes (PO3, PO5, PO7, and O1). The right CDA was calculated by subtracting ERP of right-arrowed trials (ipsilateral) from ERP of left-arrowed trials (contralateral) and then averaged it across all right electrodes (PO4, PO6, PO8, and O2).

2.4 | iTBS intervention

Subjects received two rTMS sessions in a random order with an interval of 9 months (due to the impact of COVID-19). Each rTMS session included 5 consecutive days of iTBS on a subject-specific target (peak voxel within left parietal cortex resulting from fMRI analysis) at 80% of resting-motor threshold (RMT). According to Hoy et al.'s study (2015), RMT was defined as the minimum stimulation intensity that evoked a potential from first dorsal interosseous muscle with a peak-to-peak amplitude greater than 50 μV in at least 5 out of 10 consecutive trials. To deliver iTBS, a 70 mm figure-of-eight coil connected to a Magstim Rapid2 stimulator (MagStim, Whitland, UK) was used. Briefly, iTBS was administrated as a 2 s train that repeated every 10 s for a total of 192 s. In every 2 s train, there were three pulses of stimulation given at 50 Hz, repeated every 200 ms (5 Hz). Each subject received 600 pulses in total on a single day.

During stimulation, real time stereotactic neuronavigation was implemented to ensure accurate target localization relative to each participant's neuroanatomy (Brainsight, Rogue Research). This system uses an infrared camera to monitor the positions of the subject's head and TMS coil. For each subject, a 3D model of his head was built based on his (or her) sMRI images in native space. The transformed activation image was then projected onto the model and a trajectory for the predetermined target (peaks within the left parietal cortex) was then calculated perpendicular to the skull. Reflective markers

were attached to the coil and the subject's head, so that relative positions of coil and subject's head could be tracked in real time. After coregistering to a set of anatomical locations, subject's head positions were correlated with the 3D head model, allowing precise positioning of the coil with respect to calculated trajectory. For real iTBS, the coil was placed along the trajectory with the handle being perpendicular to the long axis of the gyrus to induce posterior/anterior current flow. For sham iTBS, the coil was rotated 90° about the axis of the handle with one wing of the coil being in contact with the scalp.

2.5 | Statistical analysis

Statistical analyses were performed with the SPSS software, Version 22 (IBM Corp, New York, NY). We first used paired *t*-tests to test if the two pretests (prereal and presham) were comparable at both neural (CDA, left CDA, right CDA) and behavioral measures (*K* score). To test the effect of iTBS, we first calculated neural and behavioral changes at different iTBS conditions (for real iTBS: postreal minus prereal; for sham iTBS: postsham minus presham), which were then used as a within-subject factor (real vs. sham) in repeated-measures ANOVA. An additional within-subject factor in this analysis was task condition (3T vs. 3T2D vs. 5T). For any significant main effect of iTBS or significant interaction effect of iTBS × task, we then conducted post hoc tests using one-sample *t*-test to test the simple iTBS effect for each task condition.

To test if the iTBS effect was mainly limited within the hemisphere that received iTBS, we did a three-way repeated-measures ANOVA, in which hemisphere (left vs. right) was a within-subject factor in addition to the task condition (3T vs. 3T2D vs. 5T) and iTBS condition (real vs. sham). If hemisphere showed interactions with iTBS (e.g., significant interaction effects of hemisphere × iTBS, or hemisphere × iTBS × task), we conducted two-way repeated-measures ANOVA to identify the origin of the interactions. Additionally, one-sample *t*-tests were also performed to test the simple iTBS effect for each task condition.

Finally, we did Pearson correlation analyses on the changes of behavioral and neural measures to see if the neural effect produced by real iTBS was associated with the behavioral effect.

3 | RESULTS

No adverse events or seizures occurred during this study. Data from 22 subjects who completed two iTBS sessions were used in the final analysis.

3.1 | CDA

Three subjects were identified as outliers because their CDA amplitudes exceeded three standard deviations from the group mean and were excluded from subsequent analyses. Within the remaining 19 subjects, paired *t*-test showed that the two pretests (real-iTBS vs. sham-iTBS) were comparable (3T, $t_{18} = -0.16$, $p = .872$; 3T2D, $t_{18} = -0.41$, $p = .683$; 5 T, $t_{18} = 1.23$, $p = .235$; Table 1). When we used repeated-measures ANOVA to compare whether iTBS-related neural changes were different between the real and sham conditions, we found a significant main effect of iTBS ($F_{1,18} = 8.05$; $p = .011$). Neither the main effect of task ($F_{2,36} = 0.58$; $p = .563$) nor the interaction effect between iTBS and task ($F_{2,36} = 3.17$; $p = .054$) was significant (Table 2). Posthoc one-sample *t*-test showed significant or marginally significant results for the real iTBS condition (3T, $t_{18} = -2.13$, $p = .047$; 3 T2D, $t_{18} = -2.07$, $p = .053$; 5T, $t_{18} = -3.10$, $p = .006$), but no significant effects for the sham iTBS condition (3T, $t_{18} = -0.53$, $p = .604$; 3 T2D, $t_{18} = 0.69$, $p = .499$; 5T, $t_{18} = 1.57$, $p = .133$; Figure 3, panel b). These results revealed increased CDA (more negative) after the real iTBS intervention (Figure 3, panel a).

When CDA was analyzed by hemisphere, two of the three subjects mentioned above as outliers were again identified as outliers and their data were excluded from further analysis. For the remaining 20 subjects, the two pretests (real-iTBS vs. sham-iTBS) were also comparable (for left CDA: 3T, $t_{19} = 1.60$, $p = .126$; 3T2D, $t_{19} = 1.48$, $p = .155$; 5T, $t_{19} = 1.80$, $p = .087$; for right CDA: 3T, $t_{19} = -2.07$, $p = .053$; 3 T2D, $t_{19} = -1.19$, $p = .248$; 5T, $t_{19} = -0.97$, $p = .347$) (Table 1). Our three-way repeated-measures ANOVA using hemisphere, iTBS, and task as independent variables showed significant interaction effects of hemisphere × iTBS ($F_{1,19} = 5.59$; $p = .029$). All other effects including the interaction effects of hemisphere × iTBS × task ($F_{2,38} = 1.23$; $p = .303$) were not significant ($p > .05$). We further did a two-way repeated-measures ANOVA using iTBS and task as independent variables for the two hemispheres separately and found a significant main effect of iTBS in the left

TABLE 1 Comparisons of the pretest results between the real and sham iTBS conditions: *T* tests

	Real[a]	Sham[a]	*T* (*p*)
CDA			
3T	−1.43 (0.57)	−1.39 (1.29)	−0.16 (.872)
3T2D	−1.32 (1.02)	−1.46 (0.93)	−0.41 (.683)
5T	−1.33 (0.78)	−1.71 (1.01)	1.23 (.235)
Left CDA			
3T	−.85 (1.05)	−1.48 (1.52)	1.60 (.126)
3T2D	−.96 (1.37)	−1.65 (1.79)	1.48 (.155)
5T	−.62 (1.13)	−1.24 (1.39)	1.80 (.087)
Right CDA			
3T	−2.21 (1.45)	−1.05 (1.76)	−2.07 (.053)
3T2D	−1.96 (2.23)	−1.27 (1.39)	−1.19 (.248)
5T	−2.10 (1.32)	−1.72 (1.36)	−0.96 (.347)
K score			
3T	1.40 (0.66)	1.39 (0.91)	0.34 (.736)
3T2D	1.35 (0.50)	1.18 (1.02)	0.80 (.432)
5T	1.34 (0.07)	1.25 (0.12)	0.83 (.417)

[a]Shown as mean (*SD*).

TABLE 2 Comparisons of changes in CDA and *K*-score between the real and sham iTBS conditions: 3 tasks × 2 iTBS conditions repeated measures ANOVA

	Real[a]	Sham[a]	iTBS effect[b]	Task effect[b]	iTBS × task effect[b]
CDA					
3T	−0.48 (0.982)	−0.19 (1.530)	8.05 (.011)*	0.58 (.563)	3.17 (.054)
3T2D	−0.58 (1.226)	0.17 (1.083)			
5T	−0.77 (1.078)	0.42 (1.151)			
K-score					
3T	0.34 (0.626)	0.22 (0.969)	0.05 (.826)	4.69 (.015)*	0.48 (.623)
3T2D	0.30 (0.426)	0.38 (0.999)			
5T	0.10 (0.372)	0.01 (0.450)			

[a]Shown as mean (*SD*).
[b]Shown as *F* (*p*).
*p <.05.

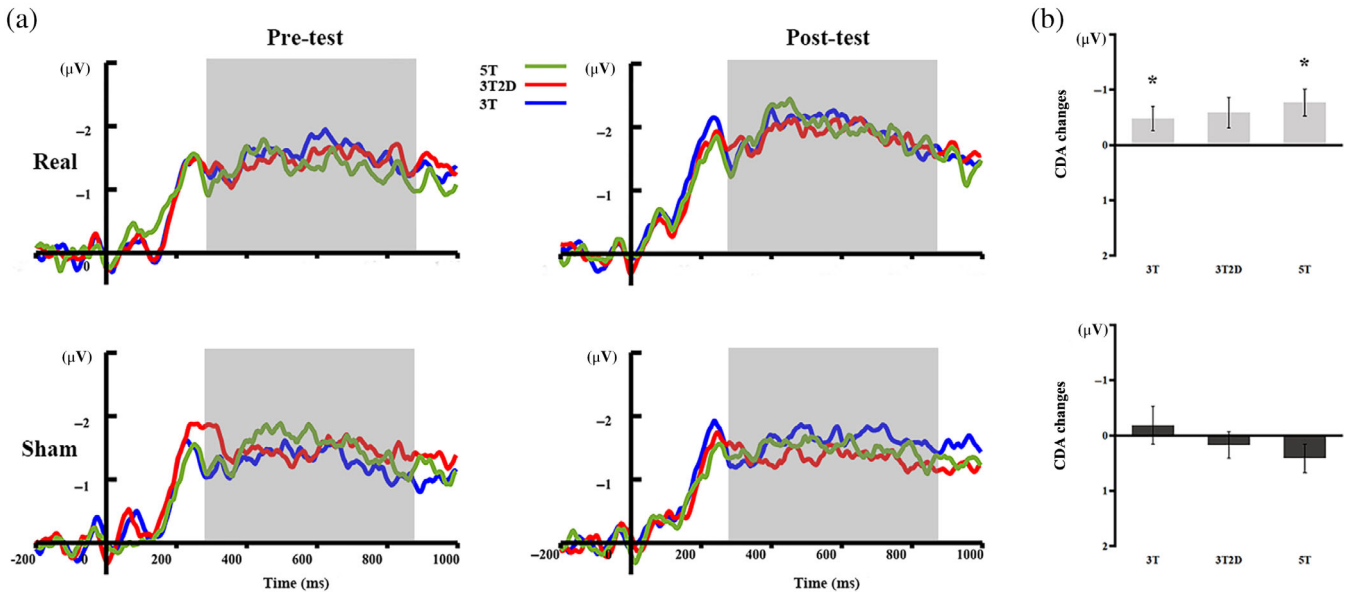

FIGURE 3 Comparisons of CDA changes between real and sham iTBS. Panel a shows CDA waveforms by task (3T, 3T2D, and 5T), iTBS condition (real and sham), and time (pre- and post-tests). The time window (300–900 ms during the delay period) is shaded. Panel b shows CDA changes induced by real and sham iTBS. Significant differences are indicated by *. Error bars indicate standard errors

hemisphere ($F_{1,19}$ = 10.53; p = .004) but not in the right hemisphere ($F_{1,19}$ = 0.76; p = .395) (Table 3). The subsequent post-hoc one-sample *t*-test in the left hemisphere showed significant results for the real iTBS condition (3T, t_{19} = −2.37, p = .029; 5T, t_{19} = −2.56, p = .019). Although the result for 3T2D was not significant, it showed a similar pattern (t_{19} = −1.71, p = .104). As for the sham iTBS, post hoc one-sample *t*-test did not find any significant result (3T, t_{19} = −0.99, p = .334; 3T2D, t_{19} = −1.67, p = .112; 5T, t_{19} = −0.23, p = .823) (Figure 4).

3.2 | *K* score

The same two subjects as mentioned above for CDA analysis by hemisphere were identified as outliers for *K* scores, so their data were excluded from subsequent analyses. We first tested whether real iTBS-generated CDA changes in the left hemisphere were correlated with *K*-score changes. As shown in Figure 5, significant or marginally significant correlations were observed (3T, r = −.46, p = .042; 3T2D, r = −.39, p = .088; 5T, r = −.66, p = .002; Figure 5).

We then tested whether real iTBS improved *K* score more than sham iTBS. Paired *t*-tests showed that the two pretests (real-iTBS vs. sham-iTBS) were comparable (3T, t_{19} = 0.34, p = .736; 3T2D, t_{19} = 0.80, p = .432; 5T, t_{19} = 0.83, p = .417; Table 1). The post hoc one-sample *t*-test revealed significant *K* score changes after real iTBS for two of the three conditions (3T: t_{19} = 2.45, p = .024; 3T2D: t_{19} = 3.10, p = .006; 5T: t_{19} = 1.32, p = .203). By contrast, sham iTBS did not change *K* score (3T: t_{19} = 1.03, p = .318; 3T2D: t_{19} = 1.68, p = .110; 5 T: t_{19} = 0.06, p = .953). However, the two-way ANOVA

TABLE 3 Comparisons of CDA changes between the real and sham iTBS conditions by hemisphere: 3 tasks × 2 iTBS conditions repeated measures ANOVA

	Real[a]	Sham[a]	iTBS effect[b]	Task effect[b]	iTBS × task effect[b]
Left hemisphere					
3T	−0.941 (1.775)	0.43 (1.920)	10.53 (.004)*	1.31 (.281)	0.23 (.792)
3T2D	−0.75 (1.959)	0.72 (1.940)			
5T	−0.97 (1.691)	0.09 (1.735)			
Right hemisphere					
3T	0.14 (2.022)	−1.11 (2.769)	0.76 (.395)	0.48 (.623)	2.41 (.104)
3T2D	−0.07 (3.130)	−0.47 (2.102)			
5T	−0.18 (2.189)	−0.07 (2.210)			

[a]Shown as mean (*SD*).
[b]Shown as *F* (*p*).
*p <.05.

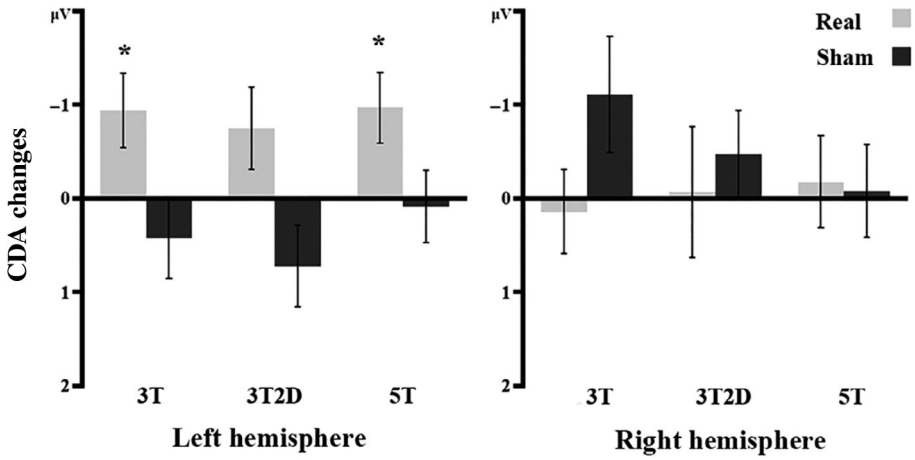

FIGURE 4 CDA changes induced by real and sham iTBS for the left hemisphere (left panel) and the right hemisphere (the right panel). Significant differences are indicated by *. Error bars indicate standard errors

that used task and iTBS as independent variables did not reveal a significant main effect of iTBS ($F_{1,19} = 0.05$; $p = .826$) or its interaction effect with task ($F_{2,38} = 0.48$; $p = .623$) on *K* score. Only the main effect of task was significant ($F_{1,19} = 4.69$; $p = .015$; Table 2).

4 | DISCUSSION

The current study, for the first time, investigated the effect of five-day individualized parietal iTBS on WM among healthy adults. Our data revealed that real iTBS (relative to sham iTBS) targeting left parietal cortex produced significantly more changes of CDA. This neural effect was more significant at the left hemisphere than at the right hemisphere. However, *K* score changes were not significantly different between real and sham iTBS, even though CDA changes were significantly correlated with *K* score changes and real iTBS (but not sham iTBS) improved *K* scores. All these results suggest that individualized repeated iTBS at the parietal cortex may improve WM based on neural measures, and that further optimization is needed to produce a behavioral effect.

The most important finding of the current study was that 5-day individualized iTBS at the parietal cortex significantly increased CDA for the 3T and 5T conditions, which indicated a positive neural effect on WM maintenance. CDA was first reported by Vogel and Machizawa (2004). In their study, when subjects performed a change detection task in which a varied number of items were bilaterally presented but only those on one side needed to be remembered, a larger negative slow wave was induced at the contralateral side (relative to the memory side) than that at the ipsilateral side. The difference between the two sides (i.e., CDA) increased with the number of items to be remembered and reached asymptote when the number of items to be remembered ($n = 4$) exceeded the WM limit. Since then, CDA has been suggested as a neural representation of WM maintenance. Later studies further identified decreased CDA in patients with certain mental disorders that are characterized by a WM maintenance deficit (Lee et al., 2010; Leonard et al., 2013). Based on these conclusions, our current finding suggests that individualized iTBS at the parietal cortex improves WM maintenance at the neural level.

However, our results showed that iTBS did not improve the other important component of WM, the interference control process, which

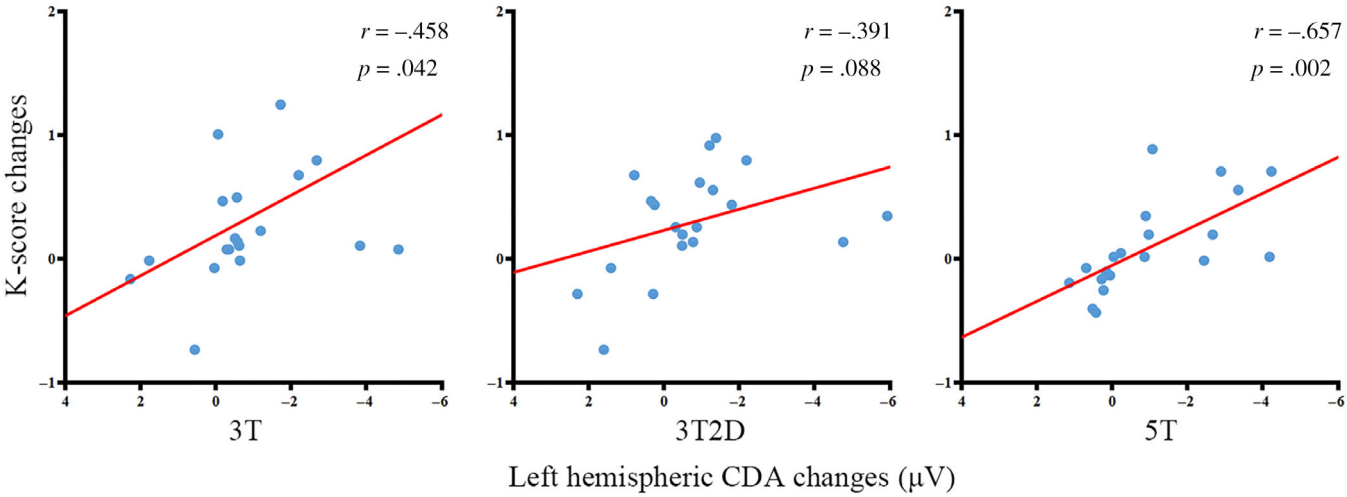

FIGURE 5 Correlations between left hemispheric CDA and *K*-score changes that were induced by real iTBS for three tasks (left panel: 3T; middle panel: 3T2D; right panel: 5T)

is the ability to efficiently exclude distractors (Vogel et al., 2005). Based on Vogel et al. (2005) and other studies (Lee et al., 2010; Spronk, Vogel, & Jonkman, 2013), interference control can be assessed by CDA differences between conditions. We found no significant iTBS-by-task interaction effect, so changes in CDA were similar across the three conditions, suggesting no effect of iTBS on interference control. Similar to our result, a recent tDCS study that tried to stimulate the parietal cortex found behavioral improvement in WM maintenance but not interference control (Li et al., 2017).

There are two plausible explanations for our results that iTBS produced significant improvement in WM maintenance but not in WM interference control. First, it may be due to the fact that iTBS of this study was administered according to individualized parietal activation during WM maintenance rather than during WM interference control. The other explanation is that the parietal cortex plays a more important role in storage than in interference control. Indeed, whether the parietal cortex plays a role in interference control is still under debate. Although the parietal cortex is responsive to the presence of distractors during WM in humans (Bomyea, Taylor, Spadoni, & Simmons, 2018; McNab & Klingberg, 2008) and animals (Suzuki & Gottlieb, 2013), researchers have argued that top-down control from other regions such as the prefrontal cortex or striatum explains the involvement of the parietal cortex in interference control (Edin et al., 2009; McNab & Klingberg, 2008). Consequently, stimulation of the parietal cortex by different kinds of physical methods has not been found to change interference control capability (Li et al., 2017).

Another interesting result of this study was that the modulatory effects of iTBS were mainly limited within the stimulated left hemisphere (but not the unstimulated contralateral cortex) and were significantly associated with behavioral changes in *K* score. Leftward asymmetry is widely demonstrated for different cognitive processes (Güntürkün, Ströckens, & Ocklenburg, 2020; Karolis, Corbetta, & Thiebaut de Schotten, 2019; Liang et al., 2021). For WM, an fMRI study found that the left (rather than the right) parietal cortex was strongly biased toward maintaining contralateral items in a load-dependent pattern, suggesting leftward asymmetry in WM (Sheremata, Bettencourt, & Somers, 2010). Consistently, patients with some neuropsychiatric diseases characterized by WM deficits have been found to show decreased leftward asymmetry (Conti et al., 2016). Some studies have further suggested that decreased leftward asymmetry is a biomarker of schizophrenia (Royer et al., 2015). Based on all the above evidence, our finding indicated that enhancing leftward asymmetry may be a possible way for the current iTBS protocol to improve WM performance.

In contrast to the significant effect of iTBS on CDA, iTBS did not show a significant effect on our behavioral results (*K*-score), even though we did find significant changes in 3T and 3T2D following real iTBS, but not following sham iTBS. One plausible explanation of the null behavioral effect is the lower sensitivity of behavioral measurement relative to ERP measurement. As a measure based on ERP, which has excellent temporal resolution, CDA can reflect brain responses during the delay period directly. This is an advantage of CDA over *K* score because brain responses during the delay period can only be postulated based on behavioral responses. In fact, several studies have suggested that CDA is more reliable than *K*-score in reflecting WM maintenance process (Gao, Ding, Yang, Liang, & Shui, 2013; Ikkai, McCollough, & Vogel, 2010; Luria, Sessa, Gotler, Jolicoeur, & Dell'Acqua, 2010; Ye, Zhang, Liu, Li, & Liu, 2014). Similar to our results, some recent rTMS studies have also reported significant effects at the ERP level rather than at the behavioral level (Chung et al., 2017; Chung, Rogasch, Hoy, & Fitzgerald, 2018; Hoy et al., 2016). It seems that detectable neural changes may precede and predict behavioral changes (Lang et al., 2020). Given the lower sensitivity of behavioral measurement, a larger sample than the current size may be needed to detect significant behavioral effects, while the current size was enough to detect significant neural effects (post hoc power >80%).

Some limitations of the current study should be mentioned. First, the dose used in this study (600 pulses per day for five consecutive days) may still be insufficient. Studies showed that application of multiple iTBS blocks has a dose-dependent effect in rodents (Volz, Benali, Mix, Neubacher, & Funke, 2013) as well as in humans (Nettekoven et al., 2014). In fact, a larger dose of rTMS (10 Hz; for 10 days with 600 pulses per day) has been applied in some previous studies (Bagherzadeh et al., 2016). Second, we only stimulated left parietal cortex, which made it impossible to determine whether iTBS improved the stimulated hemisphere or enhanced leftward asymmetry. Future research needs to explore the effect of a similar iTBS protocol on the right parietal cortex.

In conclusion, this randomized controlled study, for the first time, provides neural evidence for the effect of parietal iTBS on WM. Although this neural effect was correlated with behavioral changes, the current iTBS protocol did not produce significant behavioral improvement compared with the sham condition. These results indicate that the current iTBS protocol is a promising way to improve WM, but it needs to be further optimized in the future (e.g., involving more doses).

CONFLICT OF INTEREST

The authors declared that they have no conflict of interest.

DATA AVAILABILITY STATEMENT

The data that support the findings of this study are available from the corresponding author upon reasonable request.

ORCID

Jun Li https://orcid.org/0000-0002-9231-1791

REFERENCES

Albouy, P., Weiss, A., Baillet, S., & Zatorre, R. J. (2017). Selective entrainment of theta oscillations in the dorsal stream causally enhances auditory working memory performance. *Neuron*, *94*, 193–206. https://doi.org/10.1016/j.neuron.2017.03.015

Bagherzadeh, Y., Khorrami, A., Zarrindast, M. R., Shariat, S. V., & Pantazis, D. (2016). Repetitive transcranial magnetic stimulation of the dorsolateral prefrontal cortex enhances working memory. *Experimental Brain Research*, *234*, 1807–1818. https://doi.org/10.1007/s00221-016-4580-1

Becke, A., Müller, N., Vellage, A., Schoenfeld, M. A., & Hopf, J. M. (2015). Neural sources of visual working memory maintenance in human parietal and ventral extrastriate visual cortex. *NeuroImage*, *110*, 78–86. https://doi.org/10.1016/j.neuroimage.2015.01.059

Bomyea, J., Taylor, C. T., Spadoni, A. D., & Simmons, A. N. (2018). Neural mechanisms of interference control in working memory capacity. *Human Brain Mapping*, *39*, 772–782. https://doi.org/10.1002/hbm.23881

Brigadoi, S., Cutini1, S., Meconi1, F., Castellaro1, M., Sessa1, P., Marangon, M., … Dell'Acqua, R. (2017). On the role of the inferior intraparietal sulcus in visual working memory for lateralized single-feature objects. *Journal of Cognitive Neuroscience*, *29*, 337–351. https://doi.org/10.1162/jocn

Brunoni, A. R., & Vanderhasselt, M. A. (2014). Working memory improvement with non-invasive brain stimulation of the dorsolateral prefrontal cortex: A systematic review and meta-analysis. *Brain and Cognition*, *86*, 1–9. https://doi.org/10.1016/j.bandc.2014.01.008

Chung, S. W., Lewis, B. P., Rogasch, N. C., Saeki, T., Thomson, R. H., Hoy, K. E., … Fitzgerald, P. B. (2017). Demonstration of short-term plasticity in the dorsolateral prefrontal cortex with theta burst stimulation: A TMS-EEG study. *Clinical Neurophysiology*, *128*, 1117–1126. https://doi.org/10.1016/j.clinph.2017.04.005

Chung, S. W., Rogasch, N. C., Hoy, K. E., & Fitzgerald, P. B. (2018). The effect of single and repeated prefrontal intermittent theta burst stimulation on cortical reactivity and working memory. *Brain Stimulation*, *11*, 566–574. https://doi.org/10.1016/j.brs.2018.01.002

Constantinidis, C., & Klingberg, T. (2016). The neuroscience of working memory capacity and training. *Nature Reviews. Neuroscience*, *17*, 438–449. https://doi.org/10.1038/nrn.2016.43

Conti, E., Calderoni, S., Gaglianese, A., Pannek, K., Mazzotti, S., Rose, S., … Guzzetta, A. (2016). Lateralization of brain networks and clinical severity in toddlers with autism spectrum disorder: A HARDI diffusion MRI study. *Autism Research*, *9*, 382–392. https://doi.org/10.1002/aur.1533

Cools, R., & D'Esposito, M. (2011). Inverted-U-shaped dopamine actions on human working memory and cognitive control. *Biological Psychiatry*, *69*, e113–e125. https://doi.org/10.1016/j.biopsych.2011.03.028

Cowan, N. (2001). The magical number 4 in short-term memory: A reconsideration of mental storage capacity. *The Behavioral and Brain Sciences*, *24*, 87–114. https://doi.org/10.1017/S0140525X01003922

de Boer, N. S., Schluter, R. S., Daams, J. G., van der Werf, Y. D., Goudriaan, A. E., & van Holst, R. J. (2021). The effect of non-invasive brain stimulation on executive functioning in healthy controls: A systematic review and meta-analysis. *Neuroscience and Biobehavioral Reviews*, *125*, 122–147. https://doi.org/10.1016/j.neubiorev.2021.01.013

Delorme, A., & Makeig, S. (2004). EEGLAB: An open source toolbox for analysis of single-trial EEG dynamics including independent component analysis. *Journal of Neuroscience Methods*, *134*, 9–21. https://doi.org/10.1016/j.jneumeth.2003.10.009

D'Esposito, M., & Postle, B. R. (2015). The cognitive neuroscience of working memory. *Annual Review of Psychology*, *66*, 115–142. https://doi.org/10.1146/annurev-psych-010814-015031

Di Lazzaro, V., Pilato, F., Dileone, M., Profice, P., Oliviero, A., Mazzone, P., … Rothwell, J. C. (2008). Low-frequency repetitive transcranial magnetic stimulation suppresses specific excitatory circuits in the human motor cortex. *The Journal of Physiology*, *586*, 4481–4487. https://doi.org/10.1113/jphysiol.2008.159558

Di Lazzaro, V., Ziemann, U., & Lemon, R. N. (2008). State of the art: Physiology of transcranial motor cortex stimulation. *Brain Stimulation*, *1*, 345–362. https://doi.org/10.1016/j.brs.2008.07.004

Duncan, J., & Owen, A. M. (2000). Common regions of the human frontal lobe recruited by diverse cognitive demands. *Trends in Neurosciences*, *23*, 475–483. https://doi.org/10.1016/S0166-2236(00)01633-7

Edin, F., Klingberg, T., Johansson, P., McNab, F., Tegnér, J., & Compte, A. (2009). Mechanism for top-down control of working memory capacity. *Proceedings of the National Academy of Sciences of the United States of America*, *106*, 6802–6807. https://doi.org/10.1073/pnas.0901894106

Feredoes, E., Heinen, K., Weiskopf, N., Ruff, C., & Driver, J. (2011). Causal evidence for frontal involvement in memory target maintenance by posterior brain areas during distracter interference of visual working memory. *Proceedings of the National Academy of Sciences of the United States of America*, *108*, 17510–17515. https://doi.org/10.1073/pnas.1106439108

Gao, Z., Ding, X., Yang, T., Liang, J., & Shui, R. (2013). Coarse-to-fine construction for high-resolution representation in visual working memory. *PLoS One*, *8*, e57913. https://doi.org/10.1371/journal.pone.0057913

Goel, V., & Grafman, J. (2000). Role of the right prefrontal cortex in ill-structured planning. *Cognitive Neuropsychology*, *17*, 415–436. https://doi.org/10.1080/026432900410775

Güntürkün, O., Ströckens, F., & Ocklenburg, S. (2020). Brain lateralization: A comparative perspective. *Physiological Reviews*, *100*, 1019–1063. https://doi.org/10.1152/physrev.00006.2019

Hahn, B., Robinson, B. M., Leonard, C. J., Luck, S. J., & Gold, J. M. (2018). Posterior parietal cortex dysfunction is central to working memory storage and broad cognitive deficits in schizophrenia. *The Journal of Neuroscience*, *38*, 8378–8387. https://doi.org/10.1523/JNEUROSCI.0913-18.2018

Hamidi, M., Tononi, G., & Postle, B. R. (2008). Evaluating frontal and parietal contributions to spatial working memory with repetitive transcranial magnetic stimulation. *Brain Research*, *1230*, 202–210. https://doi.org/10.1016/j.brainres.2008.07.008

Hoy, K. E., Bailey, N., Michael, M., Fitzgibbon, B., Rogasch, N. C., Saeki, T., & Fitzgerald, P. B. (2016). Enhancement of working memory and task-related oscillatory activity following intermittent theta burst stimulation in healthy controls. *Cerebral Cortex*, *26*, 4563–4573. https://doi.org/10.1093/cercor/bhv193

Huang, Y. Z., Edwards, M. J., Rounis, E., Bhatia, K. P., & Rothwell, J. C. (2005). Theta burst stimulation of the human motor cortex. *Neuron*, *45*, 201–206. https://doi.org/10.1016/j.neuron.2004.12.033

Ikkai, A., McCollough, A. W., & Vogel, E. K. (2010). Contralateral delay activity provides a neural measure of the number of representations in visual working memory. *Journal of Neurophysiology*, *103*, 1963–1968. https://doi.org/10.1152/jn.00978.2009

Karolis, V. R., Corbetta, M., & Thiebaut de Schotten, M. (2019). The architecture of functional lateralisation and its relationship to callosal connectivity in the human brain. *Nature Communications*, *10*, 1–9. https://doi.org/10.1038/s41467-019-09344-1

Kessels, R. P. C., D'Alfonso, A. A. L., Postma, A., & De Haan, E. H. F. (2000). Spatial working memory performance after high-frequency repetitive transcranial magnetic stimulation of the left and right posterior parietal cortex in humans. *Neuroscience Letters*, *287*, 68–70. https://doi.org/10.1016/S0304-3940(00)01146-0

Lang, S., Gan, L. S., Yoon, E. J., Hanganu, A., Kibreab, M., Cheetham, J., … Monchi, O. (2020). Theta-burst stimulation for cognitive enhancement in Parkinson's disease with mild cognitive impairment: A randomized, double-blind, sham-controlled Trial. *Frontiers in Neurology*, *11*, 1–14. https://doi.org/10.3389/fneur.2020.584374

Lee, E. Y., Cowan, N., Vogel, E. K., Rolan, T., Valle-Inclán, F., & Hackley, S. A. (2010). Visual working memory deficits in patients with Parkinson's disease are due to both reduced storage capacity and impaired ability to filter out irrelevant information. *Brain*, *133*, 2677–2689. https://doi.org/10.1093/brain/awq197

Leonard, C. J., Kaiser, S. T., Robinson, B. M., Kappenman, E. S., Hahn, B., Gold, J. M., & Luck, S. J. (2013). Toward the neural mechanisms of reduced working memory capacity in schizophrenia. *Cerebral Cortex*, *23*, 1582–1592. https://doi.org/10.1093/cercor/bhs148

Li, S., Jin, J. N., Wang, X., Qi, H. Z., Liu, Z. P., & Yin, T. (2017). Theta and alpha oscillations during the retention period of working memory by rTMS stimulating the parietal lobe. *Frontiers in Behavioral Neuroscience*, *11*, 1–12. https://doi.org/10.3389/fnbeh.2017.00170

Liang, X., Zhao, C., Jin, X., Jiang, Y., Yang, L., Chen, Y., & Gong, G. (2021). Sex-related human brain asymmetry in hemispheric functional gradients. *NeuroImage*, *229*, 117761. https://doi.org/10.1016/j.neuroimage.2021.117761

Luber, B., Kinnunen, L. H., Rakitin, B. C., Ellsasser, R., Stern, Y., & Lisanby, S. H. (2007). Facilitation of performance in a working memory task with rTMS stimulation of the precuneus: Frequency- and time-dependent effects. *Brain Research*, *1128*, 120–129. https://doi.org/10.1016/j.brainres.2006.10.011

Luck, S. J., & Vogel, E. K. (1997). The capacity of visual working memory for features and conjunctions. *Nature*, *390*, 279–284. https://doi.org/10.1038/36846

Luck, S. J., & Vogel, E. K. (2013). Visual working memory capacity: From psychophysics and neurobiology to individual differences. *Trends in Cognitive Sciences*, *17*, 391–400. https://doi.org/10.1016/j.tics.2013.06.006

Luria, R., Sessa, P., Gotler, A., Jolicoeur, P., & Dell'Acqua, R. (2010). Visual short-term memory capacity for simple and complex objects. *Journal of Cognitive Neuroscience*, *22*, 496–512. https://doi.org/10.1162/jocn.2009.21214

McNab, F., & Klingberg, T. (2008). Prefrontal cortex and basal ganglia control access to working memory. *Nature Neuroscience*, *11*, 103–107. https://doi.org/10.1038/nn2024

Morgan, H. M., Jackson, M. C., Van Koningsbruggen, M. G., Shapiro, K. L., & Linden, D. E. J. (2013). Frontal and parietal theta burst TMS impairs working memory for visual-spatial conjunctions. *Brain Stimulation*, *6*, 122–129. https://doi.org/10.1016/j.brs.2012.03.001

Nettekoven, C., Volz, L. J., Kutscha, M., Pool, E. M., Rehme, A. K., Eickhoff, S. B., … Grefkes, C. (2014). Dose-dependent effects of theta burst rTMS on cortical excitability and resting-state connectivity of the human motor system. *The Journal of Neuroscience*, *34*, 6849–6859. https://doi.org/10.1523/JNEUROSCI.4993-13.2014

Oliveri, M., Turriziani, P., Carlesimo, G. A., Koch, G., Tomaiuolo, F., Panella, M., & Caltagirone, C. (2001). Parieto-frontal interactions in visual-object and visual-spatial working memory: Evidence from transcranial magnetic stimulation. *Cerebral Cortex*, *11*, 606–618. https://doi.org/10.1093/cercor/11.7.606

Pashler, H. (1988). Familiarity and visual change detection. *Perception & Psychophysics*, *44*, 369–378.

Postle, B. R., Ferrarelli, F., Hamidi, M., Feredoes, E., Massimini, M., Peterson, M., … Tononi, G. (2006). Repetitive transcranial magnetic stimulation dissociates working memory manipulation from retention functions in the prefrontal, but not posterior parietal, cortex. *Journal of Cognitive Neuroscience*, *18*, 1712–1722. https://doi.org/10.1162/jocn.2006.18.10.1712

Praß, M., & de Haan, B. (2019). Multi-target attention and visual short-term memory capacity are closely linked in the intraparietal sulcus. *Human Brain Mapping*, *40*, 3589–3605. https://doi.org/10.1002/hbm.24618

Riddle, J., Scimeca, J. M., Cellier, D., Dhanani, S., & D'Esposito, M. (2020). Causal evidence for a role of theta and alpha oscillations in the control of working memory. *Current Biology*, *30*, 1748–1754. https://doi.org/10.1016/j.cub.2020.02.065

Robitaille, N., Grimault, S., & Jolicœur, P. (2009). Bilateral parietal and contralateral responses during maintenance of unilaterally encoded objects in visual short-term memory: Evidence from magnetoencephalography. *Psychophysiology*, *46*, 1090–1099. https://doi.org/10.1111/j.1469-8986.2009.00837.x

Royer, C., Delcroix, N., Leroux, E., Alary, M., Razafimandimby, A., Brazo, P., … Dollfus, S. (2015). Functional and structural brain asymmetries in patients with schizophrenia and bipolar disorders. *Schizophrenia Research*, *161*, 210–214. https://doi.org/10.1016/j.schres.2014.11.014

Rypma, B., Prabhakaran, V., Desmond, J. E., & Gabrieli, J. D. E. (2001). Age differences in prefrontal cortical activity in working memory. *Psychology and Aging*, *16*, 371–384. https://doi.org/10.1037//0882-7974.16.3.371

Sack, A. T., Kadosh, R. C., Schuhmann, T., Moerel, M., Walsh, V., & Goebel, R. (2009). Optimizing functional accuracy of TMS in cognitive studies: A comparison of methods. *Journal of Cognitive Neuroscience*, *21*, 207–221. https://doi.org/10.1162/jocn.2009.21126

Sauseng, P., Klimesch, W., Heise, K. F., Gruber, W. R., Holz, E., Karim, A. A., … Hummel, F. C. (2009). Brain oscillatory substrates of visual short-

term memory capacity. *Current Biology*, *19*, 1846–1852. https://doi.org/10.1016/j.cub.2009.08.062

Sheremata, S. L., Bettencourt, K. C., & Somers, D. C. (2010). Hemispheric asymmetry in visuotopic posterior parietal cortex emerges with visual short-term memory load. *The Journal of Neuroscience*, *30*, 12581–12588. https://doi.org/10.1523/JNEUROSCI.2689-10.2010

Spronk, M., Vogel, E. K., & Jonkman, L. M. (2013). No behavioral or ERP evidence for a developmental lag in visual working memory capacity or filtering in adolescents and adults with ADHD. *PLoS One*, *8*, e62673. https://doi.org/10.1371/journal.pone.0062673

Suzuki, M., & Gottlieb, J. (2013). Distinct neural mechanisms of distractor suppression in the frontal and parietal lobe. *Nature Neuroscience*, *16*, 98–104. https://doi.org/10.1038/nn.3282

Todd, J. J., Marois, R., & Todd, J. J. (2004). Capacity limit of visual short-term memory in human posterior parietal cortex. *Nature*, *428*, 751–754. https://doi.org/10.1038/nature02466

Vékony, T., Németh, V. L., Holczer, A., Kocsis, K., Kincses, Z. T., Vécsei, L., & Must, A. (2018). Continuous theta-burst stimulation over the dorsolateral prefrontal cortex inhibits improvement on a working memory task. *Scientific Reports*, *8*, 1–9. https://doi.org/10.1038/s41598-018-33187-3

Vogel, E. K., & Machizawa, M. G. (2004). Neural activity predicts individual differences in visual working memory capacity. *Nature*, *428*, 748–751. https://doi.org/10.1038/nature02447

Vogel, E. K., McCollough, A. W., & Machizawa, M. G. (2005). Neural measures reveal individual differences in controlling access to working memory. *Nature*, *438*, 500–503. https://doi.org/10.1038/nature04171

Volz, L. J., Benali, A., Mix, A., Neubacher, U., & Funke, K. (2013). Dose-dependence of changes in cortical protein expression induced with repeated transcranial magnetic theta-burst stimulation in the rat. *Brain Stimulation*, *6*, 598–606. https://doi.org/10.1016/j.brs.2013.01.008

Xu, Y. (2017). Reevaluating the sensory account of visual working memory storage. *Trends in Cognitive Sciences*, *21*, 794–815. https://doi.org/10.1016/j.tics.2017.06.013

Xu, Y., & Chun, M. M. (2006). Dissociable neural mechanisms supporting visual short-term memory for objects. *Nature*, *440*, 91–95. https://doi.org/10.1038/nature04262

Yamanaka, K., Yamagata, B., Tomioka, H., Kawasaki, S., & Mimura, M. (2010). Transcranial magnetic stimulation of the parietal cortex facilitates spatial working memory: Near-infrared spectroscopy study. *Cerebral Cortex*, *20*, 1037–1045. https://doi.org/10.1093/cercor/bhp163

Ye, C., Zhang, L., Liu, T., Li, H., & Liu, Q. (2014). Visual working memory capacity for color is independent of representation resolution. *PLoS One*, *9*, e91681. https://doi.org/10.1371/journal.pone.0091681

How to cite this article: Deng, X., Wang, J., Zang, Y., Li, Y., Fu, W., Su, Y., Chen, X., Du, B., Dong, Q., Chen, C., & Li, J. (2022). Intermittent theta burst stimulation over the parietal cortex has a significant neural effect on working memory. *Human Brain Mapping*, *43*(3), 1076–1086. https://doi.org/10.1002/hbm.25708